Progress In Electromagnetics Research B, Vol. 60, 35–48, 2014

Bistatic RCS Prediction of Composite Scattering from Electrically Very Large Ship-Sea Geometry with a Hybrid Facet-Based KA and Shadow-Corrected GRECO Scheme

Mingyuan Man[1, *], Zhenya Lei[1], Yongjun Xie[2], and Xiaofeng Li[1]

Abstract—This paper presents a hybrid scheme for fast calculation on the bistatic composite scattering from electrically very large ship-sea geometry at high frequencies. Based on the Kirchhoff approximation (KA), we try to break the large-scale sea surface into myriads of plane facets, then derive the Kirchhoff integration analytically on each individual discretized facet. The analytical expression obtained, so-called the "facet-based Kirchhoff approximation (FBKA)", is suitable for a quick scattering calculation on the electrically very large sea surface, since it is beyond the intensively refined meshes as the usual Monte Carlo implementation does. Meanwhile, combined with graphical electromagnetic computing method (GRECO) to extract the illuminated and shadow facets in accordance with the incident direction, the conventional physical optics method (PO) is improved by employing current marching technique (CMT) to calculate the currents in the shadow region. The shadow-corrected GRECO is presented in this hybrid model to solve the bistatic scattering from complex and very electrically large perfectly electric conducting (PEC) objects. The accuracy of the shadow-corrected GRECO is confirmed well by exact numerical methods, especially at large scattering angles. The electromagnetic interactions between the ship and sea surface are estimated by the famous "four-path model", which has been proved to be valid for ship scattering at relatively calm sea state. Several numerical examples have been presented to demonstrate the efficiency and accuracy of the proposed hybrid method.

1. INTRODUCTION

Seeking efficient and accurate solution to the electromagnetic composite scattering from targets on sea surface has attracted much interest [1–5], which has found extensive applications in oceanic communication, radar surveillance and target detection, etc. In the analysis of composite scattering from ship-sea geometries, different numerical methods have been developed in recent years, such as the method of moment (MoM) [6–8], finite element method (FEM) [9] and finite difference time domain (FDTD) [10, 11]. In the most recent advances, iterative forward-backward method (FBM) [12, 13], generalized forward-backward method (GFBM) [14] and generalized forward-backward method (GFBM) combined with the spectrum accelerate algorithm (SAA) [15] have been proposed in succession. All the aforementioned approaches are robust and sufficiently accurate in evaluating the scattering from a two-dimensional (2-D) target on a one-dimensional (1-D) rough sea surface. However, these methods are not appropriate for solving the problem involving a three-dimensional (3-D) target on a 2-D rough sea surface due to the extremely large computational cost.

Since the multilayered media Green's function was deduced in reference [16], various approaches based on half space Green's function have been proposed to reduce the computational amounts in evaluating the scattering from ship-like objects on sea surface. Lawrence et al. [17] gave the multilevel

Received 10 February 2014, Accepted 2 May 2014, Scheduled 13 May 2014

* Corresponding author: Mingyuan Man (man-ming-yuan@163.com).

[1] National Laboratory of Antennas and Microwave Technology, Xidian University, Xi'an, Shannxi 710071, China. [2] Laboratory of Electromagnetic Compatibility, Beihang University, Beijing, China.

fast multiple algorithm (MLFMA) analysis for targets on dielectric half space interface. Xie et al. [18, 19] deduced the half space physic optic method (PO) by introducing the half space Green's function into the conventional physic optic method. Such half space Green's function based methods implicitly assume that the sea surfaces are infinite dielectric planes. Hence, these methods cannot consider the term of wind speed. When the wind speed is high, rough sea surfaces must be taken into account. Guan et al. [20] evaluated the half space Green's function on a 2-D PEC rough sea surface with Kirchhoff approximation (KA) method and further combined the method of moment (MoM) with half space Green's function to calculate the composite scattering from a 3-D object on a 2-D PEC rough sea surface. However, the surface cannot be considered as perfectly electric conducting when the frequency increases to higher than 1 GHz. Moreover, this method still may not be used to treat the scattering from electrically large ship-sea geometry for the tremendous computational cost by using the MoM.

To efficiently analyze the composite scattering from ship-sea model with appropriately dielectric rough sea surface, much effort has been paid to hybrid analytic-numerical algorithms. An electromagnetic wave(EM) scattering model based on a hybrid small perturbation method (SPM)-MoM technique was developed for the study of the EM wave interaction of a conducting object above a rough surface [21]. A hybrid KA-MoM algorithm for computation of scattering from a 3-D PEC target above a dielectric rough surface was given in reference [22, 23]. A KA-MLFMA hybrid algorithm was presented later to accelerate the hybrid KA-MoM algorithm [24]. In the aforementioned hybrid methods, the numerical methods such as SPM and KA are used to solve the scattering from the above objects and the analytic methods such as MoM and MLFMA are employed to evaluate the scattering from the below dielectric rough sea surface. These hybrid algorithms are efficient tools when the incident frequency is low. With the frequency increasing to X band or higher, the ship-like object becomes very electrically large and intractable by using MoM and MLFMA due to the poor rate of convergence and large storage requirement. In the recent literatures, high frequency methods such as shooting and bouncing ray method [25] and iterative physical optics [26] have been used to characterize the scattering from 3-D PEC object-surface geometry with low computational cost. In this case, it is reasonable to introduce high frequency methods into the hybrid analytic-numerical model which is appropriate to deal with the scattering from objects on a dielectric rough sea surface. As straightforward application of geometrical optics (GO) to flat plates and singly curved surfaces will cause difficulties in the solution procedure, it is logical to use the physical optics method (PO) to deal with the scattering from ship-like object. The conventional PO is an efficient and accurate tool to analyze the scattering of objects, but not accurate enough with the bistatic angle (which is the angle between the incident direction and the scattering direction) increases for contributions of shadow regions, especially for the case of large bistatic angles. Similarly, in the high frequency region, the randomly rough sea surface has to be generated electrically large enough, especially for the case of large observation angle (LOA). However, the rough sea surface has to be discretized with an interval distance no more than 0.2λ, where λ is the wavelength of incident wave. Hence, scattering problems of limited profile of sea surface can be treated due to terms of time consumption and memory requirement.

Considering the idea described above, in this paper, a novel hybrid algorithm combining facet-based Kirchhoff approximation (FBKA) and shadow-corrected graphical electromagnetic computing method (GRECO) is proposed to solve the composite bistatic scattering from very electrically large ship-sea geometry in high frequency region. In the research realm of rough surface scattering problems, the Kirchhoff solution is one of the most popular techniques to wave scattering from random surfaces [27, 28], and has been widely used to sea surface scattering [29, 30]. A relatively simple analytical expression of Kirchhoff solution was given by Ulaby [28]. It is convenient to use the Ulaby's equation since it removes the dependence on surface gradients by using the stationary-phase approximation during the analytical manipulation. The equation can lead to the far-field from rough surface scattering by using the height information of the meshed surface points. However, due to the presence of the highly oscillatory integral kernel, it needs to mesh the surface by 0.2λ at least during the Monte Carlo implementations, which significantly reduces the time efficiency. Since the Kirchhoff solution is based on the tangent plane approximation, we try to break the large-scale sea surface into myriads of plane facets, then derive the Ogilvy's integration analytically on each individual discretized facet. The analytical expression obtained, so-called the "facet-based Kirchhoff approximation (FBKA)", is suitable for a quick scattering calculation on the electrically very large sea surface, since it is beyond the intensively refined meshes

during the usual Monte Carlo implementation of the conventional KA. For the bistatic scattering of object at high frequencies, a hybrid method based on GRECO and current marching technique (CMT) is presented in this paper. Combined with GRECO to extract the illuminated and shadow facets in accordance with the incident direction, the conventional physical optics method (PO) is improved by employing CMT to calculate the currents in the shadow region. The demonstrated hybrid method for object can be implemented with an iterative procedure. The required number of iterations is small and does not depend on the complexity or dimension of objects. The CPU time of iterative procedure is of order N^2. These advantages imply that complex and very large objects are still tractable. Numerical results are presented and discussed in detail showing the efficiency and accuracy of this hybrid algorithm.

The paper is organized as follows. In the next section, the basic formulas of the demonstrated hybrid scheme based on facet-based KA and shadow-corrected GRECO is described in detail. In Section 3, simulation results are given to validate the accuracy and efficiency of the proposed hybrid algorithm, and In Section 4 conclusions and discussions are reported.

2. FORMULATION

2.1. Facet-based Kirchhoff Approximation (FBKA)

In deterministic Monte Carlo simulation, the sea surface is envisaged as a profile approximately decomposed by a mount of plane facets. The large-scale sea profiles are generated efficiently by the statistical wave model [31] on the basis of the Joint North Sea Wave Project (JONSWAP) sea spectrum [32]. To clarify the scattering problem, firstly we establish the coordinate system on the rough surface as illustrated in Figure 1 and define $\hat{k}^-$, A, B, C as,

$$\vec{k}^- = \hat{k}_s - \hat{k}_i, \quad A = k_X^-, \quad B = k_y^-, \quad C = k_z^- \tag{1}$$

According to the mathematical statement of the formula by Stratton and Chu, the vector formulation of the Kirchhoff scattering field from a surface can be written as follows [28],

$$E_{pq}^s\left(\hat{k}_s, \hat{k}_i\right) = -jk\frac{e^{-jkR}}{4\pi R}\hat{k}_s \times \iint_S \left[\hat{n} \times \vec{E} - \eta\hat{n} \times \left(\hat{n} \times \vec{H}\right)\right] e^{jk\left(\hat{k}_s - \hat{k}_i\right)\cdot\vec{r}} dS \tag{2}$$

$p, q = h, v$ denote the polarizations of scattering and incident wave respectively. A analytic solution has been obtained from (2) with additional simplifying assumptions, so called the stationary-phase approximation (SPA), which assumes that scattering can occur only along directions for which there are specular points on the surface.

Considering that the surface is illuminated by a unit planer wave, the scattering field by SPA is,

$$E_{pq}^s\left(\hat{k}_s, \hat{k}_i\right) = -jk\frac{e^{-jkR}}{4\pi R}\mathbb{S}_{pq}^{SPA}\iint_S e^{jk\left(\vec{k}^-\cdot\vec{r}\right)} dS \tag{3}$$

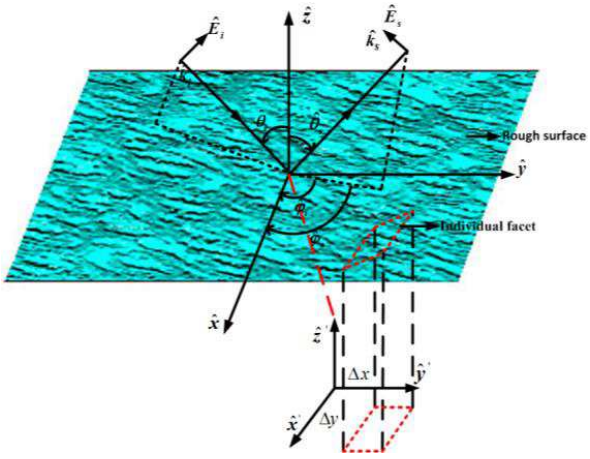

Figure 1. Geometry of sea surface scattering problem with FBKA.

where $\mathbb{S}_{pq}^{SPA}$ is polarization-dependent coefficient [28].

$$\mathbb{S}_{hh}^{SPA} = \gamma\left[\rho_{0v}\left(\hat{h}_s\cdot\hat{k}_i\right)\left(\hat{h}_i\cdot\hat{k}_s\right)+\rho_{0h}\left(\hat{v}_s\cdot\hat{k}_i\right)\left(\hat{v}_i\cdot\hat{k}_s\right)\right] \tag{4}$$

$$\mathbb{S}_{vv}^{SPA} = \gamma\left[\rho_{0v}\left(\hat{v}_s\cdot\hat{k}_i\right)\left(\hat{v}_i\cdot\hat{k}_s\right)+\rho_{0h}\left(\hat{h}_s\cdot\hat{k}_i\right)\left(\hat{h}_i\cdot\hat{k}_s\right)\right] \tag{5}$$

$$\mathbb{S}_{hv}^{SPA} = \gamma\left[\rho_{0v}\left(\hat{h}_s\cdot\hat{k}_i\right)\left(\hat{v}_i\cdot\hat{k}_s\right)-\rho_{0h}\left(\hat{v}_s\cdot\hat{k}_i\right)\left(\hat{h}_i\cdot\hat{k}_s\right)\right] \tag{6}$$

$$\mathbb{S}_{vh}^{SPA} = \gamma\left[\rho_{0v}\left(\hat{v}_s\cdot\hat{k}_i\right)\left(\hat{h}_i\cdot\hat{k}_s\right)-\rho_{0h}\left(\hat{h}_s\cdot\hat{k}_i\right)\left(\hat{v}_i\cdot\hat{k}_s\right)\right] \tag{7}$$

$\gamma = k^{-}|C|/\{[(\hat{h}_s\cdot\hat{k}_i)^2+(\hat{v}_s\cdot\hat{k}_i)^2]kC\}$, ρ_{0v} and ρ_{0h} are the Fresnel reflection coefficients for vertical and horizontal polarization respectively; $\hat{h}_s$, $\hat{v}_s$ and $\hat{h}_i$, $\hat{v}_i$ are the polarization vectors of scattering and incident waves.

The integration in (2) can be evaluated directly by using the height information of the meshed surface points. However, due to the presence of the highly oscillatory integral kernel, it needs to mesh the surface by 0.2λ (the wavelength of incident wave) at least during the Monte Carlo implementations. In this case, discretization of sea surface will cause extremely large computational burden. This kind of direct Monte Carlo implementation is involved as the "Conventional KA" in the description of this paper.

According to the Kirchhoff solution, the scattering field from each rough facet on sea surface is calculated on the basis of the tangent plane approximation, which assumes that the main contribution is from the tangent plane on the specular point. Therefore the sea surface is discretized with a sequence of dielectric planar facets and the scattering field of each facet is determined by its local incident angular and slope. To analyze the scattering from any individual facet more conveniently, we establish another coordinate as illustrated in Figure 1. With a simple application of KA method to individual facet, the scattering of any facet can be given analytically as:

$$E_{pq}^{facet}\left(\hat{k}_s,\hat{k}_i\right) = -jk\frac{e^{-jkR}}{4\pi R}\mathbb{S}_{pq}^{SPA}I \tag{8}$$

where

$$\begin{aligned} I &= e^{jk[Ax_0+By_0+Cz_0]}\iint_s e^{jk[Ax+By+C(Z_xx,Z_yy)]}dxdy \\ &= e^{jk[Ax_0+By_0+Cz_0]}\Delta x\Delta y\mathrm{sinc}\left(k\frac{\Delta x}{2}X_1\right)\mathrm{sinc}\left(k\frac{\Delta y}{2}X_2\right) \end{aligned} \tag{9}$$

and

$$X_1 = A + CZ_x \tag{10}$$

$$X_2 = A + CZ_y \tag{11}$$

(x_0, y_0, z_0), Z_x and Z_y are the center and slopes along x and y directions of each facet respectively. It should be pointed out that, when calculate $\mathbb{S}_{pq}^{SPA}$ on a tilted facet, the Fresnel reflection coefficient ρ_{0v} and ρ_{0h} used should be determinate by the local incident angles. Therefore, the scattering of sea E_{sea} can be easily obtained by summing up the contributions of all individual facets. With the demonstrated facet-based KA, the surface can be discretized with an interval distance more than 1.5λ, which implies that the demonstrated algorithm can save tremendous CPU time and memory requirement.

2.2. Shadow-Corrected Greco

2.2.1. Bistatic Scattering in Illuminated Region

In this section, shadow-corrected graphical electromagnetic computing method (GRECO) [33] is presented to calculate the bistatic scattering of ship-like object at high frequencies. The geometry of shadow-corrected GRECO for bistatic scattering is illustrated in Figure 2. Consider the idea that the GRECO can automatically and quickly eliminate the shadow regions, leading to advantages of little cost, high precision and not varying with complexity and dimensions of objects. In this paper,

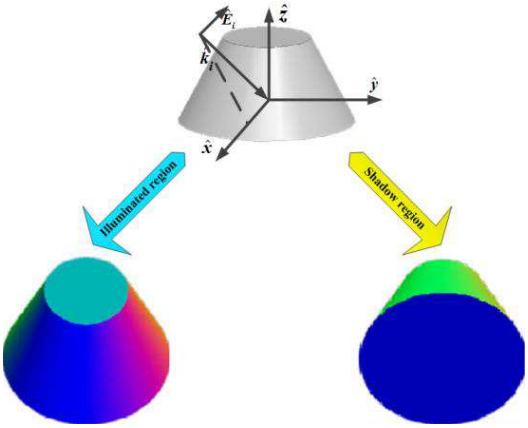

Figure 2. Geometry of shadow-corrected GRECO for bistatic scattering.

combined with GRECO to extract the illuminated and shadow facets in accordance with the incident direction by displaying lists technology of OpenGL, the scattering from illuminated region is analyzed by physical optics method (PO) accelerated by GRECO. Meanwhile, the scattering from shadow region are calculated by using current marching technique to eliminate the error of bistatic scattering obtained by the direct application of PO to objects.

To deal with the complex electrically large object, it is reasonable to assume that the incident frequency is sufficiently high so that the corresponding wavelength is small compared to the physical dimensions of the object. Combining the high frequency theory and the proper boundary conditions, we can evaluate the appropriate surface currents by applying physical optics approximations over the illuminated surface.

$$J(\bar{r}') \approx 2\hat{n} \times H_i \tag{12}$$

where $\hat{n}$ is the outward surface unit normal and H_i is the polarization unit vectors for incident magnetic field.

Applying the far-field approximation to the electric field integral equation and discretizing the surface of object, the scattered field of illuminated region can be obtained as the following expression:

$$E_{sl} = \sum_{n=1}^{N} \frac{jk}{2\pi} \frac{\exp(-jkr) E_i}{r} \hat{s} \times \left[\hat{s} \times \left(\hat{n} \times \hat{h}_i\right)\right] \exp\left[jk(\hat{s} - \hat{i}) \cdot \bar{r}'\right] \Delta s_n \tag{13}$$

where E_{sl} is the scattered field due to the illuminated facet's surface, N is the number of illuminated facets, K is the wave number of free space, $\hat{e}_i$ and $\hat{h}_i$ are the polarization unit vectors for incident electric and magnetic fields respectively, $\hat{i}$ and $\hat{s}$ are the incident and scattered propagation unit vectors respectively. Note that the surface integral is only integrated over the illuminated region.

2.2.2. Bistatic Scattering in Shadow Region

To obtain an accurate bistatic scattering of a complex and very electrically large object, the scattering from shadow region cannot be ignored. In this paper, the scattering from the shadow region is treated by employing current marching technique (CMT), which requires very limited additional computational cost.

Based on the dual surface integral equation, current marching technique [34] evaluates the currents of shadow facets uniquely by a Gauss-Seidel iteration, which calculate successive induced currents with local operators forward and backward relative to the direction of the incident wave until convergence is achieved. These local operators are defined as:

$$J_N(r) = 2n \times h_i + 2n \times \sum_{j=1}^{N} J\left(r'_j\right) \times \int_{s_j} \mathrm{grad}_{r'}\left(G\left(r, r'\right)\right) dS\left(r'\right) \tag{14}$$

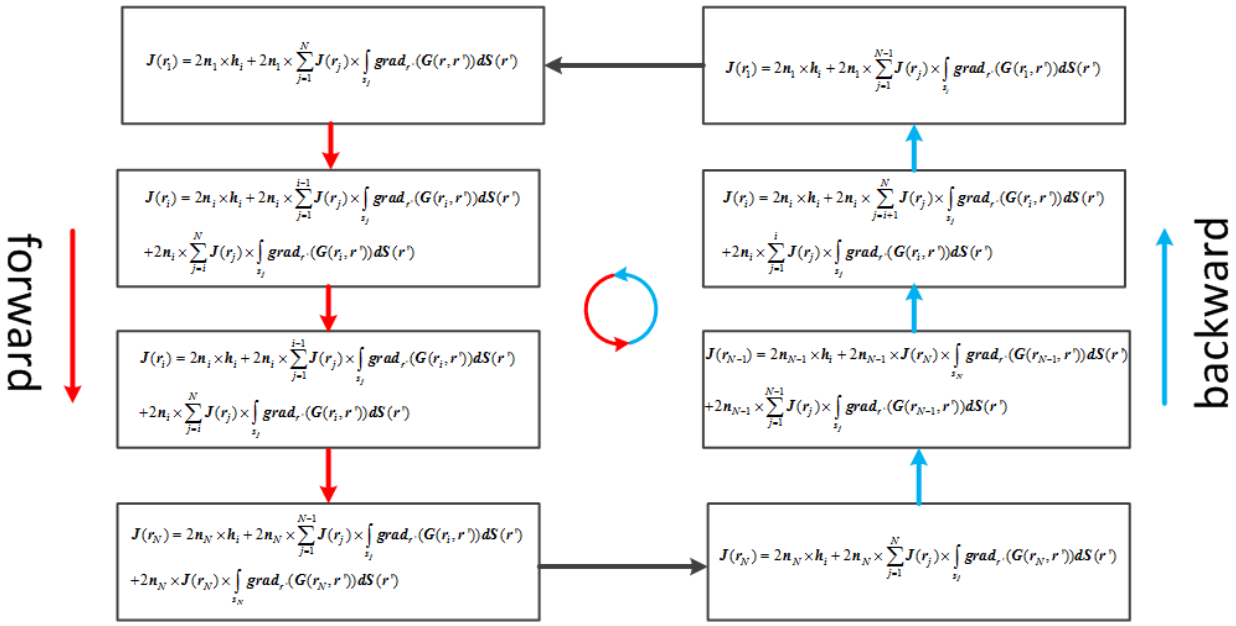

Figure 3. Procedure of current marching technique.

As illustrated in Figure 3, the forward and backward iterations are implemented by applying these local operators repeatedly to points with increasing and decreasing ranges, respectively. The currents are updated at successive ranges, replaced by the currents induced by the new magnetic field values before that range (or after the range) and the old field values after that range (or before that range), corresponding to the forward operators and backward operators respectively.

In the high frequency region, the currents mainly distribute on the illuminated region and the currents on the shadow region are very small. Based on the conventional high frequency method, however, the currents on the shadow region are assumed to be zero. In this case, the currents on the illuminated region can be regarded as reradiating a secondary electromagnetic wave and the currents on the shadow region can be appropriately regarded as coupling contributions of the currents on the illuminated region.

$$J(r) = 2n \times \sum_{j=1}^{N} J\left(r_j\right) \times \int_{s_j} \operatorname{grad}_{r'}\left(G(r, r')\right) dS\left(r'\right) \tag{15}$$

Substituting (15) into (13) and summing up the contributions from all discretized cells on the shadow region, the scattered electric field of the shadow region E_{sd} can be easily obtained.

The advantages of the shadow-corrected GRECO are described as follows. The required number of iterations is small and does not depend on the complexity or dimension of object. The CPU time of iterative procedure is of order N^2. These advantages indicate that complex and very electrically large objects are still tractable. In order to balance the efficiency and the accuracy, a single forward iteration is implemented simply.

It should be pointed out that conventional physical optics method (PO) is an accurate tool for calculation of monostatic scattering in the high frequency region. However, the calculation error of conventional PO in evaluating the bistatic scattering will increases with the bistatic angle (which is the angle between the incident direction and the scattering direction) increasing from 0° to 180°. Considering the idea described above, as a single forward iteration is implemented, it is necessary to introduce a corrected actor $\left|\sin(\frac{\theta_{bistatic}}{2})\right|$ to correct the scattered field from shadow region.

Hence, the bistatic RCS of a ship-like object can be calculated appropriately.

$$E_{ship} = E_{sl} + E_{sd}\left|\sin\left(\frac{\theta_{bistatic}}{2}\right)\right| \tag{16}$$

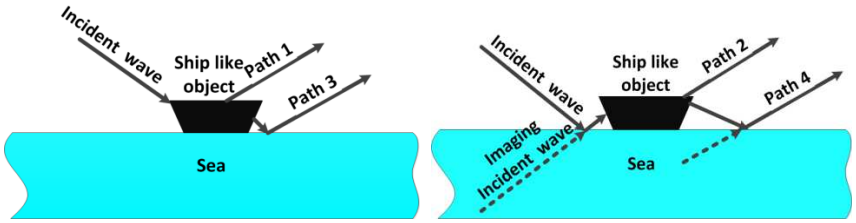

Figure 4. The four-path model.

2.3. Composite Scattering of Ship-Sea Model

The composite scattering of ship-sea model includes the contributions from the objects, the sea, and the coupling between them.

$$\sigma = 4\pi \lim_{R\to\infty} R^2 |E_{sea} + E_{ship} + E_{couple}|^2 \Big/ |E_{in}|^2 \tag{17}$$

Calculation of E_{sea} and E_{ship} have been solved in the previous parts in this paper. Due to the critical requirement of memory and CPU time for the accurately iterative evaluation of interactions between the ship and the sea, the four-path model [35] has been proved to consider the primary scattering mechanisms and is regarded as one of the most efficient schemes. The four-path model can be further simplified with a quasi-image method.

Figure 4 shows the mechanisms of the four-path model combined with a quasi-image method. It can be seen that the coupling scattered fields consists of three components corresponding to path 2–4.

$$E_{couple} = E_{os}^{second} + E_{so}^{second} + E_{sos}^{third} \tag{18}$$

where E_{os}^{second} denotes the scattering contribution of the second target-surface interaction, E_{so}^{second} denotes the scattering contribution of the second surface-target interaction and E_{sos}^{third} denotes the scattering contribution of the third target-surface-target interaction.

Combined with the quasi-image method, the solution of the coupling scattering contribution can be further simplified by utilizing image radars and image objects to simulate the electromagnetic wave reflection on the dielectric rough sea, only with a coherent reflection coefficient r which has been given in reference [36].

$$E_{couple} = rE_{i-s'}^{ship} + rE_{i'-s}^{ship} + r^2 E_{i'-s'}^{ship} \tag{19}$$

where E^{ship} represents the scattering contribution from ship; the term i' and s' in the subscripts represent the mirror image direction of the incident i and the scattering direction s respectively.

3. NUMERICAL RESULTS AND DISCUSSION

To demonstrate the advantages of the proposed hybrid algorithm, numerical examples are given in this section. The sea surface is generated with Monte Carlo method by Joint North Sea Wave Project (JONSWAP) wave spectrum. 10 randomly generated sea surface realizations are sampled for each simulation. In the following simulations, except for special declaration, the configurations of simulations are set as shown in Table 1. Only TM (vertically polarization) polarized case is considered due to the limited length of paper.

Table 1. Configurations of simulation.

Incident wave			Sea surface			
Frequency	Elevation angle θ	Azimuth angle ϕ	dimensions	temperature	Salinity	Wind direction
10 GHz	40°	0°	$200\lambda \times 200\lambda$	20°C	35‰	toward the $-x$

(Note that λ is the wavelength of incident wave)

To better validate the facet-based Kirchhoff approximation (FBKA), we carry out the comparison on a planar domain firstly. The scattering of a $20\lambda \times 20\lambda$ perfectly electric conducting plane are calculated with different algorithms. To analyze the scattering of plane by using the FBKA, assume that the $20\lambda \times 20\lambda$ plane is a facet. As illustrated in Figure 5(a), the scattering obtained by a direct application of FBKA to the plane shows a good agreement with the ones obtained by the software FEKO using the physical optics method (PO) (discretized by 0.125λ). However, we cannot obtain an accurate scattering by conventional KA when the plane is discretized by 0.625λ and 1.25λ, which verifies the efficiency of FBKA. Note that the error in the scattering of plane increases with increasing interval distance of discretization. Furthermore, the real and imaginary parts of the electric field at a distance of 500λ are shown in Figure 5(b), and the results calculated by the direct application of FBKA to the plane and by FEKO using physical optics method (discretized by 0.125λ) prove that there is no error in the phase of scattering by the demonstrated FBKA compared with the physical optics method.

It is of interest to use the proposed facet-based Kirchhoff approximation (FBKA) to calculate the bistatic scattering of a sea surface, compared to the direct application of conventional PO. For these examples, the wind speed is 5 m/s; the sea surface is discretized with equal intervals at 1.5625λ and at 0.09765625λ corresponding to FBKA and conventional KA respectively; the frequencies of incident wave are 0.5 GHz and 10 GHz respectively in Figure 6(a) and Figure 6(b). Note that the results obtained by the FBKA show a good agreement with the ones obtained by conventional KA in a wide frequency band. However, it should be pointed out that the results obtained by conventional KA are obviously

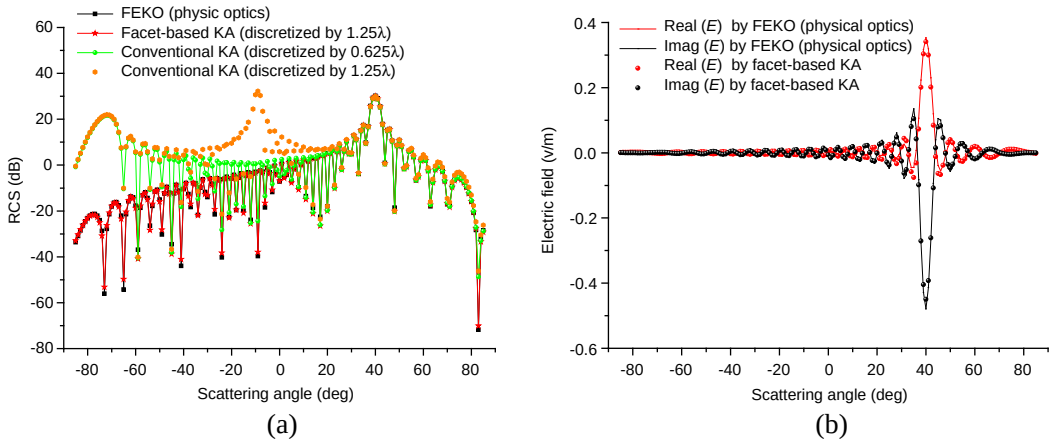

Figure 5. Validation of facet-based KA in a planar domain. (a) RCS. (b) Electric filed.

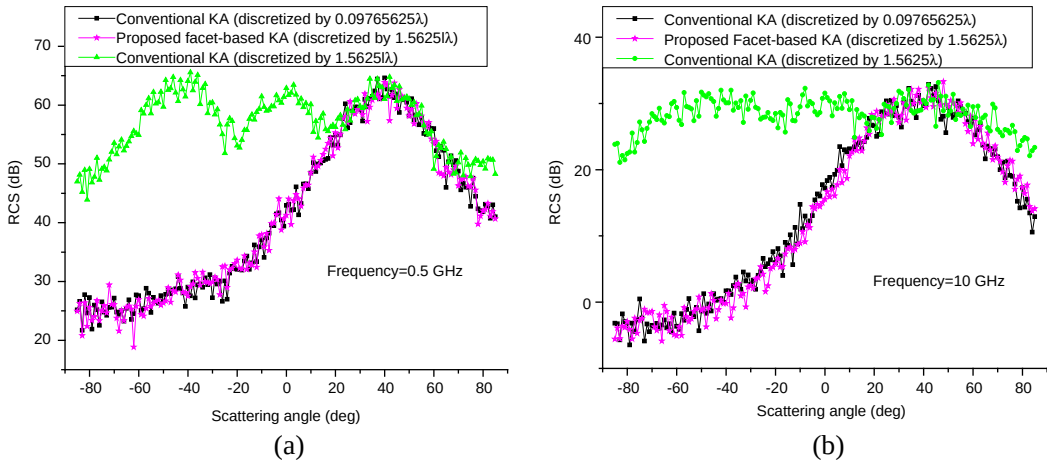

Figure 6. Comparison between facet-based KA and conventional KA for bistatic scattering of sea surface. (a) Frequency = 0.5 GHz. (b) Frequency = 10 GHz.

wrong when the surface is discretized by 1.5625λ. As illustrated by case 1 in Table 2, the memory requirement and time consumption for the demonstrated FBKA are only 1.9% and 2.2% of those for conventional KA, respectively.

Figure 7 illustrates the wind speed impact on the bistatic scattering of rough sea surface by using facet-based KA. It is found that with the wind speed increasing from 5 m/s to 15 m/s, the bistatic scattering in the specular direction will decrease, and the back scattering will increase. The results are reasonable as the diffused scattering of sea surface will be stronger with the wind speed increasing.

To verify the efficiency and accuracy of the proposed shadow-corrected graphical electromagnetic computing method (GRECO), a sphere and a flare (ship-like geometry) are chosen as two typical examples to be simulated. The geometries are illustrated in Figure 8 and Figure 9, respectively. For

Table 2. Comparison for memory and CPU time.

	Incident frequency (GHz)	Methods	CPU time (s)	Memory (MB)
Case 1	0.5 and 10.0	Facet-based KA	559	2
		Conventional KA	25595	105
Case 2	10.0	Shadow-corrected GRECO (for sphere)	1052	84
		MLFMA (for sphere)	3182	1113
		Shadow-corrected GRECO (for flare)	1449	87
		MLFMA (for flare)	5224	1059
Case 3	1.0	Facet-based KA + shadow-corrected GRECO	4974	87.4
		Conventional KA + MLFMA	28366	1577.7

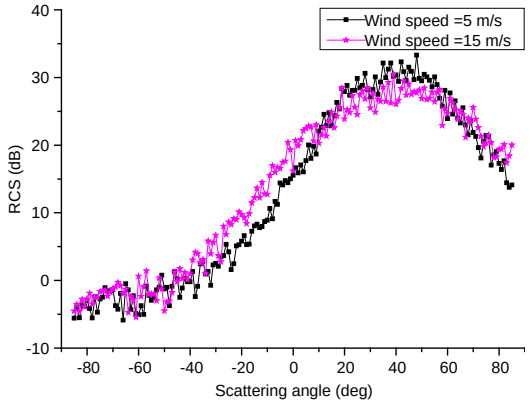

Figure 7. Wind speed impact on bistatic scattering of rough sea surface.

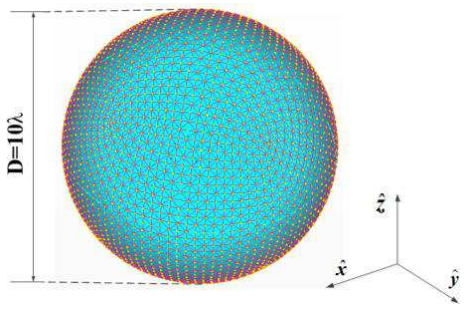

Figure 8. Geometry of sphere.

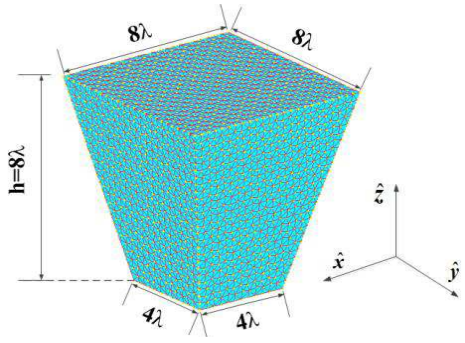

Figure 9. Geometry of flare.

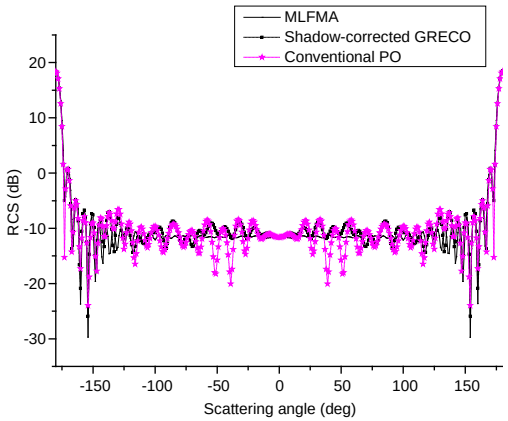

Figure 10. Comparison between shadow-corrected GRECO, MLFMA and conventional PO for bistatic scattering of a sphere.

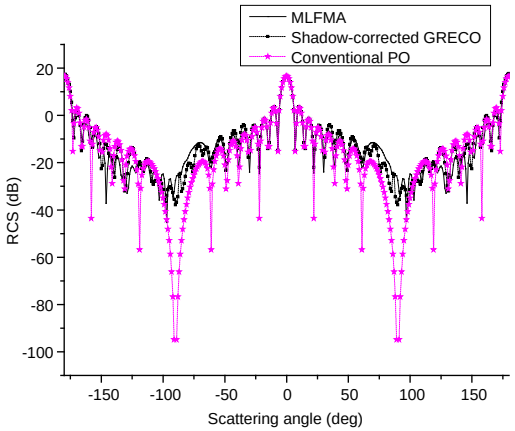

Figure 11. Comparison between shadow-corrected GRECO, MLFMA and conventional PO for bistatic scattering of a flare.

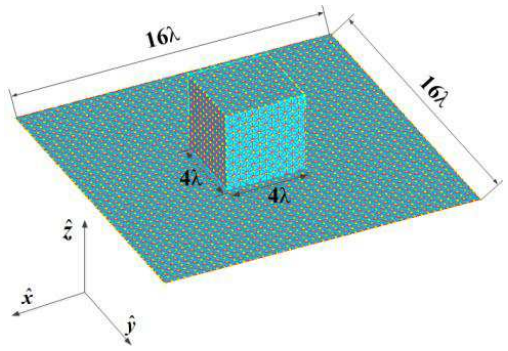

Figure 12. Geometry of a cube on a plane.

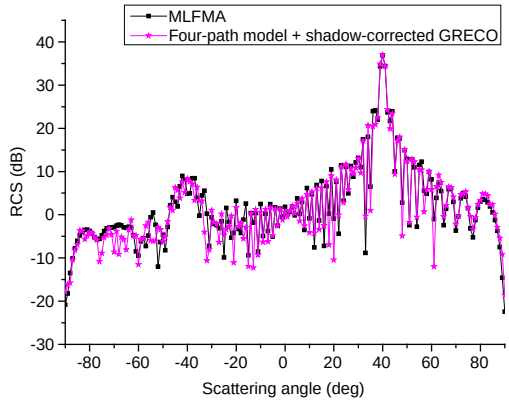

Figure 13. Comparison between four-path model + shadow-corrected GRECO and MLFMA for bistatic scattering of a cube on a plane.

these examples, both the sphere and flare are discretized by 0.33λ and 0.125λ corresponding to shadow-corrected GRECO and multilevel fast multiple algorithm (MLFMA) respectively. The elevation angle θ of incident wave is 0°. It can be seen in Figure 10 and Figure 11 that the results obtained with the proposed shadow-corrected GRECO agree well with the ones evaluated by using MLFMA. As shown in Figure 10 and Figure 11, in the direction of backscattering, the scattering of both sphere and flare obtained by conventional physical optics method (PO) agree well with the ones obtained by MLFMA as the contributions of currents in the illuminated region dominate the monostatic scattering at high frequencies. The impact of the currents in the shadow region is weak. However, in other directions, there is obvious difference between the results obtained by conventional PO and MLFMA due to the contributions of currents in the shadow region. Considering the contribution of current in shadow region, the results obtained with the proposed shadow-corrected GRECO agree well with the ones evaluated by using MLFMA.

However, as illustrated by case 2 in Table 2, for the geometry of sphere, the memory requirement and CPU time by using shadow-corrected GRECO are only 8.2% and 33.1% of those by MLFMA, respectively; for the geometry of flare, the memory requirement and CPU time by using shadow-corrected GRECO are only 1.9% and 27.7% of those by GRECO, respectively. It can be concluded that the demonstrated method can cut down the memory requirement and time consumption greatly

compared to MLFMA.

As illustrated in Figure 13, the bistatic scattering of the PEC geometry in Figure 12 obtained by the hybrid four-path method and shadow-corrected GRECO agrees well with the one using MLFMA. We reach the conclusion that shadow-corrected GRECO can give the accurate scattering of objects, so it can be concluded that the four-path method can give sufficiently accurate scattering of coupling interactions between ship and rough sea surface, and the four-path method is reasonable.

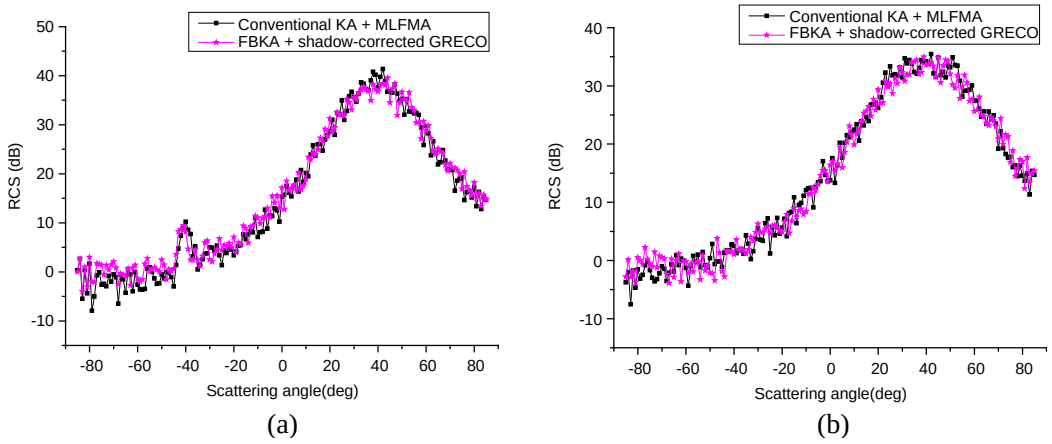

Figure 14. Comparison between facet-based KA + shadow-corrected GRECO and conventional KA + MLFMA for bistatic scattering of a ship-like object on sea surface. (a) Wind speed = 3 m/s. (b) Wind speed = 5 m/s.

For validating the demonstrated hybrid facet-based Kirchhoff approximation (FBKA) and shadow-corrected GRECO scheme, the composite scatterings of an $8\lambda \times 8\lambda \times 8\lambda$ cube on a rough sea surface obtained by the novel hybrid scheme are compared with those by a hybrid conventional KA and method of moment (MoM) (accelerated by MLFMA). For these examples, the wind speeds are 3 m/s and 5 m/s, respectively in Figure 14(a) and Figure 14(b). The sea surface and the cube are discretized with the same intervals as in Figure 6 and Figure 8, respectively. Considering the critical requirement of memory and CPU time by using MLFMA, the frequency is set at 1 GHz. Firstly the results obtained by the demonstrated hybrid method show good agreement with the results by using a hybrid conventional KA and MoM (accelerated by MLFMA) algorithm. In addition, as shown in Figure 14(a), a peak back scattering of the comprehensive geometry is located around -40° due to the strong interactions between the ship-like object and sea surface when the wind speed is low at 3 m/s. The ship and rough sea surface are combined into a dihedral structure, However, when the wind speed increases to 5 m/s in Figure 14(b), the specular scattering of sea surface decreases, and the diffuse scattering of sea surface increases, making the interactions between the ship-like object and sea surface weak. There is no peak value of the backscattering meaning that the object is masked by the roughened sea surface, which is logical.

The memory requirement and time consumption using the novel hybrid method are only 5.5% and 17.5% of those by a hybrid conventional KA and MoM (accelerated by MLFMA) scheme respectively as shown in case 3 in Table 2, which indicates that the novel hybrid scheme can cut down the computational cost significantly.

The last example is a ship located on an 80 m × 80 m rough sea surface depicted in Figure 15. The configurations of this simulation list as follows: the incident frequency is 10 GHz, the elevation angle $\theta = 40^\circ$, the azimuth angle $\phi = 0^\circ$; 10 randomly generated sea surface realizations are sampled, the wind speed is 3 m/s, the sea surface is meshed by 0.3125 meter. From Figure 16, it can be found that all the backscattering in the direction from -90° to 0° is enhanced greatly and two peaks are located around -10° and -70° due to the strong coupling interactions between ship and sea. The forward scattering is mainly determined by the scattering of sea surface, except for the specular direction where the bistatic scattering of the ship at high frequency is large enough to dominate the composite scattering.

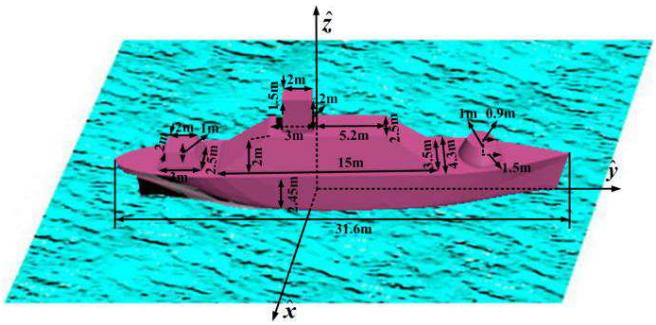

Figure 15. Geometry of a ship on rough sea surface.

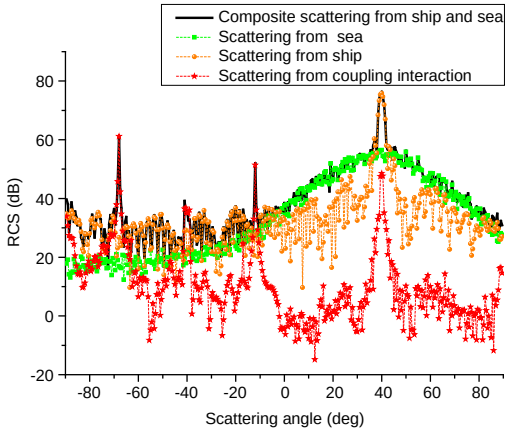

Figure 16. Bistatic scattering of different contributions (wind speed = 3 m/s).

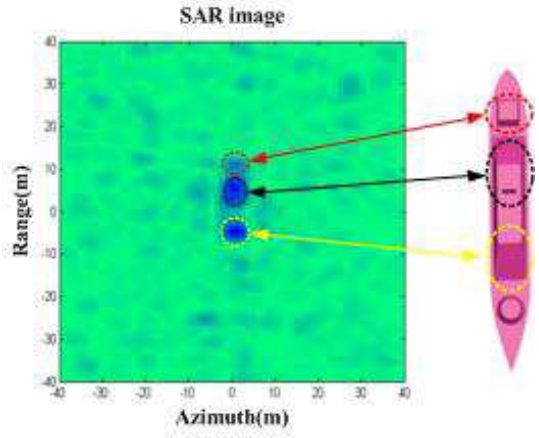

Figure 17. SAR image of comprehensive ship-sea geometry (HH polarization, $\theta = 60°$).

To further validate the novel hybrid scheme, considering the idea in reference [37], a synthetic aperture radar(SAR) image of the comprehensive ship-sea geometry for HH polarization is given in Figure 17. The incident frequency remains 10 GHz; the bandwidth of the base band is 50 MHz; the elevation angle θ of incident wave is 60° and other parameters are the same as in Figure 16. The ship can be clearly seen from the background of sea surface validating the accuracy of the novel scheme again.

4. CONCLUSIONS

Based on the most popular four-path method, a novel hybrid facet-based KA and shadow-corrected GRECO method is presented in this paper to evaluate the bistatic composite scattering from electrically very large ship-sea geometry at high frequencies. To obtain a quick solution of scattering problem from the electrically very large sea surface, we derive the Ogilvy's integration analytically on each individual discretized facet and give the analytical expression of facet-based Kirchhoff approximation which beyond the intensively refined meshes during the usual Monte Carlo implementation of the conventional KA. The FBKA can significantly cut down the memory requirement and CPU time compared to conventional KA. Combined with GRECO to extract the illuminated and shadow facets in accordance with the incident direction, a hybrid algorithm based on conventional physical optics method for the illuminated region and current marching technique for the shadow region is presented to accurately solve the bistatic scattering from complex and electrically very large PEC objects, especially for the case of large scattering angles. Promising results demonstrate that this hybrid method can accurately and efficiently evaluate the bistatic composite scattering of electrically very large ship-sea geometry.

REFERENCES

1. Jin, Y. Q., "Advances in numerical simulation of composite scattering from target above rough surface," *9th International Symposium on Antennas Propagation and EM Theory (ISAPE)*, 806–809, 2010.
2. Baussard, A., M. Rochdi, and A. Khenchaf, "PO/MEC-based scattering model for complex objects on a sea surface," *Progress In Electromagnetics Research*, Vol. 111, 229–251, 2011.
3. Zhang, M., W. Luo, G. Luo, C. Wang, and H. C. Yin, "Composite scattering of ship on sea surface with breaking waves," *Progress In Electromagnetics Research*, Vol. 123, 263–277, 2012.
4. Ji, W. J. and C. M. Tong, "Bistatic scattering from two-dimensional dielectric ocean rough surface with a PEC object partially embedded by using the G-SMCG method," *Progress In Electromagnetics Research*, Vol. 105, 119–139, 2010.
5. Wu, Z. S., J. J. Zhang, and L. Zhao, "Composite electromagnetic scattering from the plate target above a one-dimensional sea surface: Taking the diffraction into account," *Progress In Electromagnetics Research*, Vol. 92, 317–331, 2009.
6. Wang, X., C. F. Wang, Y. B. Gan, and L. W. Li, "Electromagnetic scattering from a circular target above or below rough surface," *Progress In Electromagnetics Research*, Vol. 40, 207–227, 2003.
7. Ku, H. C., R. S. Awadallah, R. L. McDonald, and N. E. Woods, "Fast and accurate algorithm for electromagnetic scattering from 1-D dielectric ocean surfaces," *IEEE Trans. Antennas Propag.*, Vol. 54, No. 8, 2381–2391, 2006.
8. Guo, L. X., A. Q. Wang, and J. Ma, "Study on EM wave scattering from 2-D target above 1-D large scale rough surface with low grazing incidence by parallel MoM based on PC clusters," *Progress In Electromagnetics Research*, Vol. 89, 149–166, 2009.
9. Ozgun, O. and M. Kuzuoglu, "Monte carlo-based characteristic basis finite-element method (MC-CBFEM) for numerical analysis of scattering from objects on/above rough sea surfaces," *IEEE Trans. Geosci. Remote Sens.*, Vol. 50, No. 3, 769–783, 2012.
10. Li, J. and L. X. Guo, "FDTD investigation on the bistatic scattering from a target above two-layered rough surfaces using UPML absorbing condition," *Progress In Electromagnetics Research*, Vol. 88, 197–211, 2008.
11. Li, J. and L. X. Guo, "Investigation on wide-band scattering of a target above randomly rough surface by FDTD method," *Optics Express*, Vol. 19, No. 2, 1091–1100, 2011.
12. Holliday, D., L. L. DeRaad, and G. J. St-Cyr, "Forward-backward: A new method for computing low-grazing angle scattering," *IEEE Trans. Antennas Propag.*, Vol. 44, No. 5, 722–729, 1996.
13. Li, Z. X. and Y. Q. Jin "Numerical simulation of bistatic scattering from a fractal rough surface using the forward backward method," *Electromagnetics*, Vol. 22, No. 3, 191–207, 2002.
14. Rodriguez Pino, M., L. Landesa, J. L. Rodriguez, F. Obelleiro, and R. J. Burkholder, "The generalized forward-backward method for analyzing the scattering from targets on ocean-like rough surfaces," *IEEE Trans. Antennas and Propag.*, Vol. 47, No. 6, 961–969, 1999.
15. Li, Z. X. and Y. Q. Jin, "Bistatic scattering from a fractal dynamic rough sea surface with a ship presence at low grazing-angle incidence using the GFBM/SAA," *Microw. Opt. Techn. Let.*, Vol. 31, No. 2, 146–151, 2001.
16. Michalski, K. A. and J. R. Mosig, "Multilayered media Green's functions in integral equation formulations," *IEEE Trans. Antennas Propag.*, Vol. 45, No. 3, 508–519, 1997.
17. Liu, Z. J., J. Q. He, Y. J. Xie, A. Sullivan, and L. Carin, "Multilevel fast multipole algorithm for general targets on a half-space interface," *IEEE Trans. Antennas Propag.*, Vol. 50, No. 12, 1838–1849, 2002.
18. Li, X. F., Y. J. Xie, P. Wang, and T. M. Yang, "High-frequency method for scattering from electrically large conductive targets in half-space," *IEEE Antennas Wireless Propaga. Lett.*, Vol. 6, 259–262, 2007.
19. Li, X. F., Y. J. Xie, and R. Yang, "High-frequency method for scattering from coated targets with electrically large size in half space," *IET Microwaves, Antennas & Propagation*, Vol. 3, No. 2, 181–186, 2009.

20. Guan, B., J. F. Zhang, X. Y. Zhou, and T. J. Cui, "Electromagnetic scattering from objects above a rough surface using the method of moments," *IEEE Trans. Geosci. Remote Sens.*, Vol. 47, No. 10, 3399–3405, 2009.
21. Zhang, Y., Y. E. Yang, H. Braunish, and J. A. Kong, "Electromagnetic wave interaction of conducting object with rough surface by hybrid SPM/MoM technique," *Journal of Electromagnetic Waves and Applications*, Vol. 13, No. 7, 983–984, 1999.
22. Ye, H. X. and Y. Q. Jin, "A hybrid analytic-numerical algorithm of scattering from an object above a rough surface," *IEEE Trans. Geosci. Remote Sens.*, Vol. 45, No. 5, 1174–1180, 2007.
23. Zhang, X. Y. and X. Q. Sheng, "An efficient hybrid KA-MoM method for scattering from objects above a rough surface," *Asia-Pacific Microwave Conference*, 16–20, Dec. 2008.
24. Yang, W., W. Yang, Z. Q. Zhao, C. H. Qi, W. Liu, and Z. P. Nie, "Iterative hybrid method for electromagnetic scattering from a 3-D object above a 2-D random dielectric rough surface," *Progress In Electromagnetics Research*, Vol. 17, 435–448, 2011.
25. Li, J., L. X. Guo, Q. He, and R. W. Xu, "Characterization of 3D electromagnetic scattering from PEC man-made target above rough surface," *Microwave and Millimeter Wave Technology (ICMMT)*, Vol. 2, 1–4, 2012.
26. Li, J., B. Wei, Q. He, L. X. Guo, and D. B. Ge, "Time-domain iterative physical optics method for analysis of EM scattering from the target half buried in rough surface: PEC case," *Progress In Electromagnetics Research*, Vol. 121, 391–408, 2011.
27. Beckmann, P. and A. Spizzichino, *The Scattering of Electromagnetic Waves from Rough Surfaces*, Pergamon, New York, 1963.
28. Ulaby, F. T., R. K. Moore, and A. K. Fung, *Microwave Remote Sensing, Volume II*, Addison-Wesley Publishing Company, Canada, 1982.
29. Barrick, D. E., "Rough surface scattering based on the specular point theory," *IEEE Trans. Antennas Propag.*, Vol. 16, No. 4, 449–454, 1968.
30. Hesany, V., W. J. Plant, and W. C. Keller, "The normalized radar cross section of the sea at 10° incidence," *IEEE Trans. Geosci. Remote Sens.*, Vol. 38, No. 1, 64–72, 2000.
31. Tessendorf, J., "Simulating ocean water. Simulating nature: Realistic and interactive techniques," ACM SIGGRAPH 2001 Course Notes #47, 2001.
32. Hasselmann, K., et al., "Measurements of wind-wave growth and swell decay during the Joint North Sea Wave Project (JONSWAP)," Repository Hydraulic Engineering Reports, Deutsches Hydrographisches Institut, Hamburg, 1973.
33. Rius, J. M., M. Ferrando, and L. Jofre, "High-frequency RCS of complex radar targets in real-time," *IEEE Trans. Antennas Propag.*, Vol. 41, No. 9, 1308–1319, 1993.
34. Zaporozhets, A. A. and M. F. Levy, "Bistatic RCS calculation with the vector parabolic equation method," *IEEE Trans. Antennas Propag.*, Vol. 47, 1688–1696, 1999.
35. Johnson, J. T., "A numerical study of scattering from an object above a rough surface," *IEEE Trans. Antennas Propag.*, Vol. 50, No. 10, 1361–1367, 2002.
36. Wang, Y. and X. J. Xu, "On wideband radar signature simulation of ships over sea surface," *Acta Aeronautica et Astronautica Sinica*, Vol. 30, No. 2, 337–342, 2009.
37. Franceschetti, G., M. Migliaccio, and D. Riccio, "On ocean SAR raw signal simulation," *IEEE Trans. Geosci. Remote Sens.*, Vol. 36, No. 1, 84–100, 1998.